Front. Phys. 13(1), 130201 (2018)
DOI 10.1007/s11467-017-0698-2

RESEARCH ARTICLE

Mean-field approximations of fixation time distributions of evolutionary game dynamics on graphs

Li-Min Ying[1], **Jie Zhou**[1], **Ming Tang**[2], **Shu-Guang Guan**[1], **Yong Zou**[1,†]

[1] *Department of Physics, East China Normal University, Shanghai 200062, China*
[2] *School of Information Science Technology, East China Normal University, Shanghai 200241, China*
Corresponding author. E-mail: †*yzou@phy.ecnu.edu.cn*

Received March 2, 2017; accepted April 27, 2017

The mean fixation time is often not accurate for describing the timescales of fixation probabilities of evolutionary games taking place on complex networks. We simulate the game dynamics on top of complex network topologies and approximate the fixation time distributions using a mean-field approach. We assume that there are two absorbing states. Numerically, we show that the mean fixation time is sufficient in characterizing the evolutionary timescales when network structures are close to the well-mixing condition. In contrast, the mean fixation time shows large inaccuracies when networks become sparse. The approximation accuracy is determined by the network structure, and hence by the suitability of the mean-field approach. The numerical results show good agreement with the theoretical predictions.

Keywords fixation time distribution, complex networks, coordination game

PACS numbers 02.50.Ey, 87.23.Kg, 02.50.Ga

1 Introduction

Frequency-dependent selection processes are traditional models for evolutionary game theory [1, 2]. Previously, these models have been mainly concentrated on well-mixed populations [3], which are based on the so-called replicator equation describing the variations of frequencies of the strategies in the population [2]. Deterministic replicator equations are helpful to understand the dynamics of infinite, homogeneous, and well-mixed populations. In a population of two strategies, fixation refers to the probability for one strategy to take over the entire population, causing the extinction of the other strategy [4]. In structured populations, fixation appears as a consequence of spatial constraints because the underlying governing dynamics are stochastic [4, 5]. More specifically, assuming that a population has N players and that s_1 and s_2 are two strategies for each player, the quantity of interest in this evolutionary process is the fixation probability that ends up in a state of N s_1-players given an initial state of n s_1-players (out of N players). Obviously, the characteristic timescales also play a crucial role in fixations because they might occur very slowly or rapidly [5, 6].

Recently, many results have uncovered the importance of heterogeneous population structures on individuals strategy updating behaviors [5, 7]. In particular, much progress has focused on game models on complex networks [8, 9]. Faced with finite-sized populations of heterogeneous connectivity patterns, stochastic approaches have been employed to investigate the dynamic process of fixation [4, 10–15]. The difference between deterministic and stochastic modeling was further compared in Refs. [16–18], and systematically shown in Ref. [19]. Other factors that are important for fixations include noise effects [20–23], population structures, and spatial constraints [24–26].

To characterize the fixation processes, we need to compute the probabilities of fixations and to determine their associated timescales. Concerning the speed of fixations, one important quantity that the majority of existing studies have focused on is the computation of mean fixation time that the system needs to reach the final absorbing state. We emphasize that, in many cases, the mean fixation time can provide good estimates [13, 27]. However, it has been recently shown that the mean fixation time is insufficient when the distributions of fixation

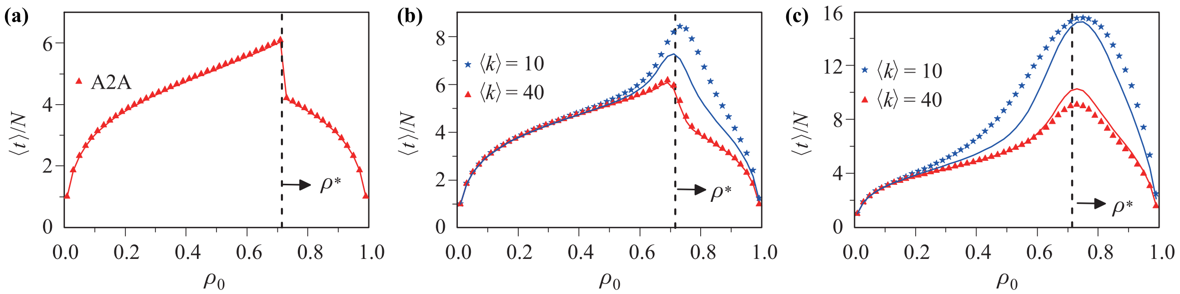

Fig. 1 Mean fixation times $\langle t\rangle/N$ to pure s_1-players in pairwise comparison processes, depending on the initial density ρ_0. The payoff matrix is $a_{11} = 1.2$, $a_{12} = 0$, $a_{21} = 0.8$, $a_{22} = 1$ and $\kappa = 0.1$. The dots are numerical simulations, while the solid lines are from the theory. The network size is $N = 100$ in all cases, **(a)** all-to-all connected (well mixed, A2A) population, **(b)** Erdos–Renyi (ER) random networks, and **(c)** scale-free networks. In (b, c), the network mean degree $\langle k\rangle = 40(\blacktriangle)$, $10(\star)$.

times are broad or skewed [28, 29]. As shown in Fig. 1, the theoretical estimation of the mean fixation times demonstrates large deviations from numerical simulations. This becomes particularly pronounced when simulating coordination game dynamics on networks and, for instance, the initial frequency of one type of player is close to the unstable interior point. Recently, an alternative has been to compute the distribution of fixation times in terms of the spectrum in eigenspace [29]. More specifically, they have proposed to construct eigenspace representations of the original fixation time distributions, which reduced the computation to forward-only processes in each time step.

In this work, we study the effects of network structures on fixation by implementing game models on Erdos–Renyi (ER) random networks and scale-free networks, compared the case of all-to-all connected N nodes. As it is known, a complex network is a convenient way to represent the heterogeneous interacting population structure in human society [9]. Various network dynamics have been studied on top of a complex network, including synchronization and epidemic spreading processes, among others [8, 9, 30–35]. The degree k measures the connections node i has and the mean degree of the network is $\langle k\rangle$. Currently, it remains unknown how the network size N and mean degree $\langle k\rangle$ influence the distribution functions of fixation times, the clarification of which will be the task of this work.

This paper is organized as follows: In Section 2, we introduce the basics for the game models on complex networks, and point out the inaccuracies of the numerical estimation of the mean fixation times. The general stochastic framework is proposed in Section 3, explicitly showing the distribution functions of fixation times. In this section, we also revisit the mean fixation times and all m-order moments of the distribution functions. We numerically show the accuracy of our theories to estimate the distribution functions of fixation times in Section 4. The conclusions are summarized in Section 5.

2 Problem statement

Game model and strategy updating rules: Population structure is introduced into the game models by assuming that strategy updating is only possible between connected nodes [8, 11]. More specifically, we consider that each link represents a game and the two nodes attached to this link are two players in the game. The number of games in which a player participates varies over the population because the nodes of the network have potentially different degrees k. We assume that each link of the network represents a symmetric two-player game and the payoff matrix is expressed as

$$\mathcal{A} = \left(\begin{array}{c|cc} & s_1 & s_2 \\ \hline s_1 & a_{11} & a_{12} \\ s_2 & a_{21} & a_{22} \end{array}\right). \tag{1}$$

Each player has two strategies, either s_1 or s_2. Depending on the payoff matrix $\mathcal{A}$, there are four generic cases [11]: (i) Dominance. Either s_1 dominates s_2 ($a_{11} > a_{21}$ and $a_{12} > a_{22}$) or s_2 dominates s_1 ($a_{11} < a_{21}$ and $a_{12} < a_{22}$), for instance, prisoner's dilemma; (ii) bistability ($a_{11} > a_{21}$, $a_{22} > a_{12}$); (iii) coexistence ($a_{11} < a_{21}$ and $a_{12} > a_{22}$); and (iv) neutrality ($a_{11} = a_{21}$ and $a_{12} = a_{22}$).

An initial fraction ρ_0 of s_1 players is assigned randomly and time is divided into discrete periods. After one iteration step, the payoff of player i is accumulated from all games in which i is involved in i's neighborhood. A proper strategy updating rule is introduced before moving to the next step. There are many updating rules in the literature, most of which are based on imitation and learning [8, 36, 37]. In this work, we consider a pairwise comparison (Fermi process) of synchronized updating rule [11], which is as follows:

The payoff u_i is accumulated in the neighborhood of i as $u_i = \sum_{l=1, l\in\mathcal{N}_i}^{N} A_{il} s_i \mathcal{A} s_l$, where $\mathcal{A}$ is the payoff matrix and $\mathcal{N}_i$ is the set of neighbors of node i. At the end of each iteration, player i decides whether to keep its current action or to adopt the action of one of its neighboring players j, depending on the current payoff difference between i and j, $u_i - u_j$. Then, player i randomly selects one neighbor j from its neighborhood $\mathcal{N}_i$ and switches to j's action in the next round with a probability

$$w_{s_i \to s_j} = \frac{1}{1 + \mathrm{e}^{(u_i - u_j)/\kappa}}, \tag{2}$$

where κ denotes the noise amplitude characterizing the level of rationality of individuals, which is often chosen as $\kappa = 0.1$ following previous works [36]. A smaller κ corresponds to a stronger influence of j on i. The larger the payoff difference between i and j, the higher probability i tends to adopt j's action in the next round.

Fixation probabilities and fixation times: In a well-mixed population where each individual is equally likely to interact with any other individual, the density of individuals adopting the strategy of s_1 is denoted by ρ (or equivalently, frequency of s_2 players is $1 - \rho$) [10]. In the case of coordination games, there are three equilibrium points: two absorbing boundary points $\rho = 0$ and $\rho = 1$, and one unstable interior fixed point ρ^*, which reads

$$\rho^* = \frac{a_{22} - a_{12}}{a_{11} + a_{22} - a_{12} - a_{21}}. \tag{3}$$

Note that the system is bistable and the stable state $\rho = 0$ is separated from $\rho = 1$ by ρ^*. For initial frequencies above ρ^*, the population evolves toward 100% of pure s_1 individuals, namely, $\rho = 1$ [10, 17]. On the contrary, the system is absorbed to $\rho = 0$ if $\rho_0 < \rho^*$, showing an abrupt transition at ρ^*. In the case in which s_2 dominates s_1 (i.e., prisoner's dilemma), the only stable equilibrium is $\rho = 0$ because s_2 is a Nash equilibrium and therefore, $\rho = 0$ is an evolutionarily stable strategy.

To characterize the evolutionary process, one often uses the fixation probability B that the system reaches the absorbing boundary at $\rho = 1$, and the corresponding asymptotic expectation times $\langle t \rangle$. We note that the finite size N of the populations and the underlying network structures are crucial to the dynamics [19]. In our previous work [19], we mainly focused on the fixation probabilities B. However, as demonstrated in Fig. 1, we find there are large deviations in the mean fixation times when the initial densities of s_1-players (ρ_0) are close to the unstable fixed point ρ^*. This discrepancy becomes larger when considering network structures, for instance, scale-free networks [Fig. 1(c)], and the mean degrees (connectivity) of networks [Fig. 1(d)].

3 Theory

Without loss of generality, we suppose that at time t, the probability to have n nodes out of N players with s_1 strategy is $\phi_n = f(n, t)$. There are $N + 1$ possible states $\phi_0, \phi_1, \cdots, \phi_n, \cdots, \phi_N$. The network state at time t is hence represented by a vector $f(\boldsymbol{n}, t) = (f(0, t), f(1, t), \cdots, f(n, t), \cdots, f(N, t))$, which fulfills the normalization $\sum_{n=0}^{N} f(n, t) = 1$. There are two absorbing states: (i) $f(0, t)$ corresponds to the case of 0 players with strategy s_1 (or all are s_2 players), and (ii) $f(N, t)$ means that the whole network is full of s_1 players. The network state at time $t + 1$ is represented by

$$f(\boldsymbol{n}, t + 1) = f(\boldsymbol{n}, t)M, \tag{4}$$

where M is the transition matrix of the network state. In the next step, we study the dynamics based on M.

We start in the situation of the well-mixing limit. At time step t, we assume there are n out of N players with s_1 strategy. Therefore, the payoffs of each strategy are as follows:

$$u_{s_1} = a_{11}n + a_{12}(N - n), \tag{5}$$

$$u_{s_2} = a_{21}n + a_{22}(N - n). \tag{6}$$

Furthermore, we define the frequency of s_1 players as $\rho = n/N$,

$$u_{s_1} = N[a_{11}\rho + a_{12}(1 - \rho)], \tag{7}$$

$$u_{s_2} = N[a_{21}\rho + a_{22}(1 - \rho)]. \tag{8}$$

We assume that, in the neighborhood of node i, there is a fraction n/N of players in state s_1. Namely, at time t, we have

$$\rho_i = \frac{\#\{s_1 \text{ players in } \mathcal{N}_i\}}{k} \triangleq \rho = \frac{n}{N}, \tag{9}$$

where $\mathcal{N}_i$ and k are the neighborhood and degree of node i, respectively. Under the mean-field assumption, we replace N with $\langle k \rangle$ in Eqs. (7) and (8) in the following analysis.

3.1 Transition probabilities and mean fixation times

Before obtaining the distribution functions of fixation times, we follow our previous stochastic approach in obtaining the mean fixation times on complex networks [19]. Note that the previous work [19] only considered coordination game models. In this work, we assume that there are two absorbing states and derive the unconditional fixation time distributions. Our numerical results will be performed on different games models, including coordination and prisoner's dilemma models.

Note that there are no differences in the results below if one replaces the subscript s_1 by s_2; therefore, we omit these in the following. In the next round $t + 1$, the transition (hopping) probability that the number of s_1 players is increased to $n + 1$ is expressed as

$$T_+(n) = (1 - \rho)\rho \sum_{k=0}^{\infty} P(k) \sum_{k'=0}^{\infty} P(k'|k) w(u_k^+, u_{k'}^+), \tag{10}$$

where k is the degree of node i; $P(k)$ is the probability to have a node of degree k; $P(k'|k)$ is the conditional probability that a link from a node of degree k points to a node of degree k'; and $w(u_k^+, u_{k'}^+)$ is the probability to switch to s_1 in the next round where u_k^+ is the payoff of degree k when taking action of s_2 and $u_{k'}^+$ is the payoff of degree k' when taking action of s_1. More specifically,

$$w(u_k^+, u_{k'}^+) = 1/\{1 + \exp[(u_k^+ - u_{k'}^+)/\kappa]\}, \tag{11}$$

$$u_k^+ = k[\rho a_{21} + (1-\rho)a_{22}], \quad u_{k'}^+ = k'[\rho a_{11} + (1-\rho)a_{12}]. \tag{12}$$

When obtaining Eq. (10), we assume that the strategy updating of player i is independent of its degree k. The mean-field approximation further requires that the variance of the degree sequence k_i is small; for instance, the mean degree of a network $\langle k\rangle$ should not be too small. Our numerical simulations below show that sparser networks of small values of $\langle k\rangle$ show good agreement with the theoretical predictions as well.

In a full analogy, in the next iteration $t+1$, the transition probability that the number of s_1 players is decreased to $n-1$ reads

$$T_-(n) = \rho(1-\rho)\sum_{k=0}^{\infty} P(k) \sum_{k'=0}^{\infty} P(k'|k) w(u_k^-, u_{k'}^-), \tag{13}$$

where $w(u_k^-, u_{k'}^-)$ is the probability to switch to s_2 in the next round; in particular,

$$w(u_k^-, u_{k'}^-) = 1/\{1 + \exp[(u_k^- - u_{k'}^-)/\kappa]\}, \tag{14}$$

$$u_k^- = k[\rho a_{11} + (1-\rho)a_{12}], \quad u_{k'}^- = k'[\rho a_{21} + (1-\rho)a_{22}]. \tag{15}$$

The probability to keep n s_1-players unchanged at time $t+1$ is given by

$$T_0(n) = 1 - T_+(n) - T_-(n). \tag{16}$$

We note that $T_+(0) = T_-(N) = 0$ because the two boundary states are absorbing.

In the case of the well-mixing limit, we have $k' = k = N-1$ and $P(k') = P(k'|k) = 1$. Equations (10) and (13) are further simplified as

$$T_+(n) = (1-\rho)\rho w(u_k^+, u_{k'}^+), \tag{17}$$

$$T_-(n) = \rho(1-\rho) w(u_k^-, u_{k'}^-). \tag{18}$$

Therefore, we retrieve the results that were reported in Refs. [10, 13]. In this case, one defines the ratio of the transition probabilities as $q_n = T_-(n)/T_+(n)$, which was used to compute the average fixation times based on the recursive expression of the distributions of fixation times [13]. Here we take a different approach to compute the distribution functions of fixation times.

With $T_+(n)$ and $T_-(n)$, we obtain the transition matrix M, the details of which are provided in the Appendix. Transition matrix M of the Markov process is tridiagonal and the dimension of M is $(N+1)\times(N+1)$. Furthermore, M can be decomposed into three blocks, namely, (i) I_2 represents the absorbing states, (ii) R is the transition probability that the system reaches the absorbing states in 1 step, and (iii) Q characterizes the transition probabilities from any transient states. In our previous work [19], we have shown that the fixation probabilities and the average times that is necessary for the system to reach the absorbing states are determined by the fundamental matrix $H = (I_{N-1} - Q)^{-1}$, where I_{N-1} is the identity matrix [12]. Furthermore, we define the matrix $B = HR$, which has dimension $(N-1)\times 2$. Starting from any initial state of $n \in [1, N-1]$ s_1 players (or $N-n$ s_2 players), B_{n2} and B_{n1} are the probabilities that the system is attracted to the absorbing state of all s_1 players and all s_2 players, respectively. The two probabilities B_{n2} and B_{n1} fulfill the normalization

$$\sum_{j=1}^{2} B_{nj} = 1. \tag{19}$$

Furthermore, the mean fixation time for the system to be attracted to the absorbing state from any initial state of n s_1-players is given by

$$\langle t_n\rangle = \sum_{m=1}^{N-1} H_{nm}. \tag{20}$$

For the purpose of comparison between networks of different sizes, one normalizes it by the number of nodes in the network, namely, $\langle t_n\rangle/N$.

3.2 Unconditional fixation time distribution

When $1 \le n \le N-1$ (any transient states), the dynamic equations of the system [Eq. (4)] at time step $t+1$ are represented by

$$f(\boldsymbol{n}, t+1) = f(\boldsymbol{n}, t)Q. \tag{21}$$

The stochastic dynamics of the network are described by the master equation as

$$\frac{\Delta f(\boldsymbol{n}, t)}{\Delta t} = f(\boldsymbol{n}, t+1) - f(\boldsymbol{n}, t). \tag{22}$$

Substituting Q [Eq. (A2) in Appendix A] into the above Eq. (22), we have

$$\frac{\Delta f(\boldsymbol{n}, t)}{\Delta t} = f(\boldsymbol{n}, t)(Q - I_{N-1}). \tag{23}$$

In the limit of $\Delta t \to 0, N \to \infty$ and the notation of the fundamental matrix $H = (I_{N-1} - Q)^{-1}$, we have

$$\frac{\mathrm{d}f(\boldsymbol{n}, t)}{\mathrm{d}t} = -f(\boldsymbol{n}, t)H^{-1}, \tag{24}$$

and the solution reads

$$f(\boldsymbol{n},t) = f(\boldsymbol{n},0)\mathrm{e}^{-H^{-1}t}. \tag{25}$$

Therefore, the attraction of the transient state to the absorbing state of $n = 0$ (all are s_2 players) in one step, to the absorbing state of $n = N-1$ (all are s_1 players), is represented by

$$\frac{f(0,t)}{\mathrm{d}t} = f(1,t)T_-(1) = T_-(1)[f(\boldsymbol{n},0)\mathrm{e}^{-H^{-1}t}]_{1,1}, \tag{26}$$

$$\frac{f(N,t)}{\mathrm{d}t} = f(N-1,t)T_+(N-1)[f(\boldsymbol{n},0)\mathrm{e}^{-H^{-1}t}]_{1,N-1}. \tag{27}$$

Thus, the probability for the transient state to be attracted to the absorbing states is computed as

$$\begin{aligned} P_t &= \frac{f(0,t)}{\mathrm{d}t} + \frac{f(N,t)}{\mathrm{d}t} \\ &= T_-(1)[\mathrm{e}^{-H^{-1}t}]_{n,1} + T_+(N-1)[\mathrm{e}^{-H^{-1}t}]_{n,N-1}. \end{aligned} \tag{28}$$

We note that P_t describes the fixation time distribution function of the system from any initial condition of n s_1-players.

3.3 Mean fixation times: Revisited

From the distribution function Eq. (28), the mean fixation time [Eq. (20)] for the system to reach the absorbing states is alternatively expressed as follows:

$$\begin{aligned} \langle t_n \rangle &= \int_0^{+\infty} tP_t\mathrm{d}t \\ &= T_-(1)\left[\int_0^{+\infty} t\mathrm{e}^{-H^{-1}t}\mathrm{d}t\right]_{n,1} \\ &\quad + T_+(N-1)\left[\int_0^{+\infty} t\mathrm{e}^{-H^{-1}t}\mathrm{d}t\right]_{n,N-1} \\ &= T_-(1)(H^2)_{n,1} + T_+(N-1)(H^2)_{n,N-1} \\ &= T_-(1)\sum_{j=1}^{N-1} H_{nj}H_{j1} + T_+(N-1)\sum_{j=1}^{N-1} H_{nj}H_{j(N-1)} \\ &= \sum_{j=1}^{N-1} H_{nj}[T_-(1)H_{j1} + T_+(N-1)H_{j(N-1)}] \\ &= \sum_{j=1}^{N-1} H_{nj}\sum_{l=1}^{2} B_{jl}. \end{aligned} \tag{29}$$

Owing to Eq. (19) (details are in Appendix A), we have

$$\langle t_n \rangle = \sum_{j=1}^{N-1} H_{nj}\sum_{l=1}^{2} B_{jl} = \sum_{j=1}^{N-1} H_{nj}, \tag{30}$$

which has exactly the same form as Eq. (20).

3.4 Mean conditional fixation time

If one considers the fixation time to all s_1 players given an initial condition of n s_1-players, the mean conditional fixation time is derived from the distribution [Eq. (28)], which reads

$$\begin{aligned} \langle t_n^{s_1} \rangle &= \int_0^{+\infty} tP_t^{s_1}\mathrm{d}t \\ &= T_+(N-1)\frac{\left[\int_0^{+\infty} t\mathrm{e}^{-H^{-1}t}\mathrm{d}t\right]_{n,N-1}}{B_{n2}} \\ &= T_+(N-1)\frac{(H^2)_{n,N-1}}{B_{n2}}. \end{aligned} \tag{31}$$

3.5 Standard deviation and all moments

In addition, the variance σ^2 of the fixation time distribution is

$$\begin{aligned} \sigma^2 &= \langle t^2 \rangle - \langle t \rangle^2 \\ &= \int_0^{+\infty} t^2 P_t\mathrm{d}t - \left(\sum_{j=1}^{N-1} H_{nj}\right)^2 \\ &= 2(T_-(1)(H^3)_{n,1} + T_+(N-1)(H^3)_{n,N-1}) \\ &\quad - \left(\sum_{j=1}^{N-1} H_{nj}\right)^2. \end{aligned} \tag{32}$$

We obtain all moments of m-order as follows:

$$\begin{aligned} \langle t_n^m \rangle &= \int_0^{+\infty} t^m P_t\mathrm{d}t \\ &= T_-(1)\left[\int_0^{+\infty} t^m\mathrm{e}^{-H^{-1}t}\mathrm{d}t\right]_{n,1} \\ &\quad + T_+(N-1)\left[\int_0^{+\infty} t^m\mathrm{e}^{-H^{-1}t}\mathrm{d}t\right]_{n,N-1} \\ &= (m!)[T_-(1)(H^{m+1})_{n,1} + T_+(N-1)(H^{m+1})_{n,N-1}]. \end{aligned} \tag{33}$$

4 Numerical results

For better comparison purposes, we perform simulations on populations of (i) all-to-all connections, (ii) Erdos–Renyi (ER) random networks, and (iii) scale-free networks generated by the Barabási and Albert's algorithm (BA). The selection strength is $\kappa = 0.1$ for both models. The network sizes are specified in the figure captions. Initially, we randomly choose a fraction of ρ_0 from N network nodes to be s_1-players.

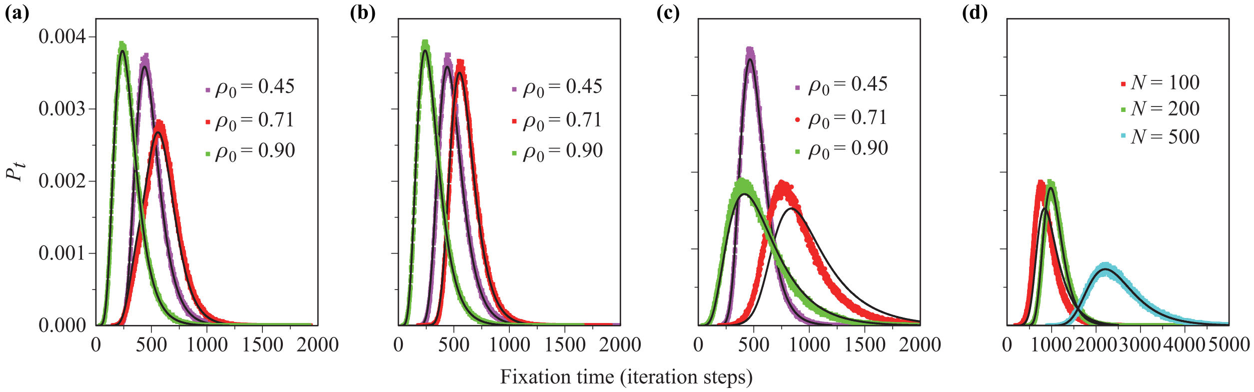

Fig. 2 Probability density functions of unconditional fixation times for coordination games. Three representative initial conditions are indicated by legends $\rho_0 = 0.45$, 0.71 (ρ^*), and 0.9. The dots are numerical simulations and the black bold lines are theoretical predictions by Eq. (28). The network sizes are $N = 100$ for (a–c): **(a)** all-to-all connected population, **(b)** ER random networks, **(c, d)** scale-free networks, **(d)** three different sizes of scale free networks $100, 200$, and 500. In (b, c, d), the network mean degree is $\langle k \rangle = 40$.

4.1 Coordination games

In the coordination game model, the payoff matrix is chosen as $a_{11} = 1.2$, $a_{12} = 0$, $a_{21} = 0.8$, and $a_{22} = 1$, such that $\rho^* \approx 0.71$. The mean fixation times, as shown in Fig. 1, suggest that the numerical estimations show large deviations from the theoretical estimations, especially when ρ_0 is close to the unstable interior point ρ^*. Therefore, we focus on the special case of $\rho_0 = 0.71$, comparing to the other two cases of initial conditions ($\rho_0 = 0.45$, and 0.9). In Fig. 2, we first show P_t [Eq. (28)] for three different values of ρ_0. The dependence of σ on ρ_0 and the mean degree of the networks $\langle k \rangle$ will be checked in Figs. 3 and 4, respectively.

Distribution functions of fixation times: We show P_t of coordination games in Fig. 2. In all cases, i.e., all-to-all connected, ER, and BA networks, P_t is shown to be asymmetric with much longer tails (Fig. 2). When $\rho_0 = 0.71$, the theoretical prediction by Eq. (28) shows large deviations from the numerical results for the BA networks. However, these discrepancies are reduced when large network sizes are used, as shown in Fig. 2(d).

Standard deviations: Depending on the initial conditions ρ_0, we show the standard deviations of fixation time distribution functions in Fig. 3. We find that there are no significant changes in σ in the well-mixing limit, as shown in Fig. 3(a). In the case of ER random networks, an increased σ has been observed only when the ρ_0 values are close to the unstable point of ρ^*. On the contrary, the σ values are significantly increased in the case of BA scale-free networks because the fixation time distribution functions are much broader than the other two cases. In addition, we find relatively large discrepancies between the numerical estimations and theoretical predictions, especially for BA networks, as shown in Fig. 3(a). It turns

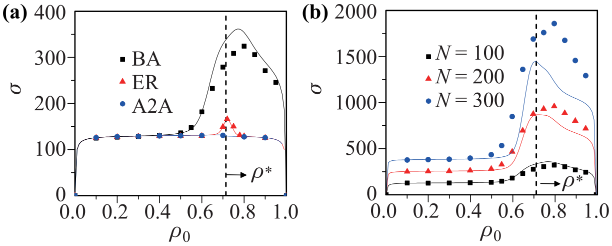

Fig. 3 Standard deviations versus initial conditions of ρ_0 for coordination games. **(a)** The network size is $N = 100$ for all-to-all connected population (●), ER random networks (▲), and BA scale-free networks (■). In both ER and BA networks, the mean degree is $\langle k \rangle = 40$. **(b)** Three different network sizes for scale-free networks: 100 (■), 200 (▲), and 300 (●). The dots are numerical simulations and the black bold lines are theoretical predictions by Eq. (32). The vertical dashed lines correspond to the position of $\rho^* = 0.71$.

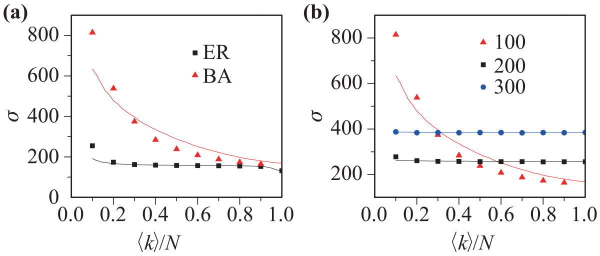

Fig. 4 Standard deviations versus networks average degrees $\langle k \rangle$ (divided by size $N = 100$) for coordination games when $\rho_0 = 0.71$. **(a)** ER random networks (▲), BA scale-free networks (■). **(b)** Three different network sizes for scale-free networks: 100 (▲) 200 (■), and 300 (●). The dots are numerical simulations and the continuous lines are theoretical predictions by Eq. (32).

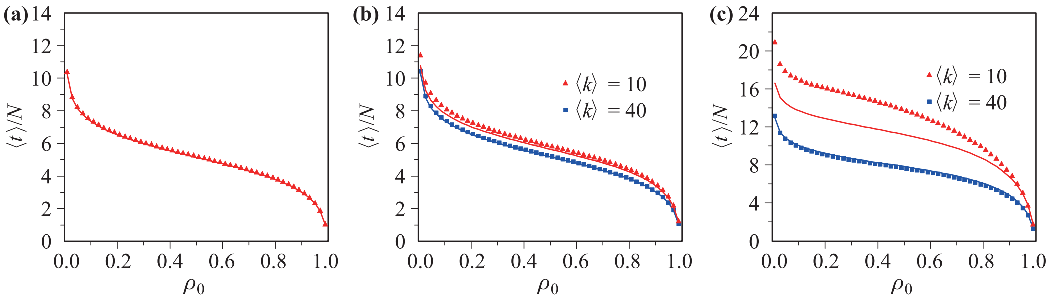

Fig. 5 Mean fixation times $\langle t\rangle/N$ to pure s_1-players in Prisoner's dilemma model. The dots are numerical simulations, while the solid lines are from the prediction [Eq. (31)]. The network size is $N = 100$ in all cases: **(a)** all-to-all connected (well-mixed) population, **(b)** ER random networks, and **(c)** scale-free networks. The mean fixation times are sufficient when networks average degrees $\langle k\rangle$ are large in both ER and scale-free networks, which are compared using $\langle k\rangle = 10$ (▲), 40 (■).

out that these discrepancies become more pronounced when the network size increases, as shown in Fig. 3(b). These discrepancies are related to a possible inadequacy of the well-mixed state assumption in the scale-free network when the analytical expression of σ is derived.

In addition, we have checked the dependence of σ on the average connectivity (degree) of networks, which is shown in Fig. 4. We conclude that the predictions by Eq. (32) do not show pronounced differences from the numerical estimations if the mean degrees $\langle k\rangle/N$ are larger than 0.2.

4.2 Prisoner's dilemma games

In the prisoner's dilemma model, we choose $a_{11} = 1.2$, $a_{12} = 1.0$, $a_{21} = 0.8$, and $a_{22} = 0$. In this case, s_2 dominates s_1 in the payoff matrix [Eq. (1)] and it is a strict Nash equilibrium. The only stable equilibrium is $\rho_{s_1} = 0$, because s_2 is an evolutionarily stable strategy while s_1 is not.

The results in Fig. 5 suggest that it may be sufficient to compute the mean fixation time to characterize the dynamic process in ER random networks, which is further supported by P_t in Fig. 6. More specifically, we show P_t in Fig. 6 for two typical initial values, $\rho_0 = 0.45$ and 0.9. In addition, Figs. 7(a, b) and (c, d) show σ depending on, respectively, the initial values ρ_0 and the mean network degrees $\langle k\rangle/N$. Based on both Figs. 6 and 7, we conclude that the mean fixation time is sufficient in the case of the prisoner's dilemma when simulations are performed on all-to-all connected populations and ER random networks. However, the numerical simulation shows relatively large deviations from the theoretical prediction in P_t in BA networks, particularly when $\rho_0 = 0.9$ [Fig. 6(b)].

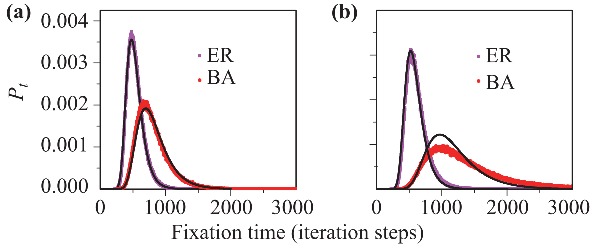

Fig. 6 P_t for prisoner's dilemma games on ER and BA networks, where the networks mean degrees are $\langle k\rangle = 40$ and the network size is $N = 100$ in both cases. **(a)** $\rho_0 = 0.45$ and **(b)** $\rho_0 = 0.9$. The black lines are from the theory.

5 Conclusions

Simulations of game models on top of complex networks show that mean fixation times $\langle t\rangle$ are often insufficient

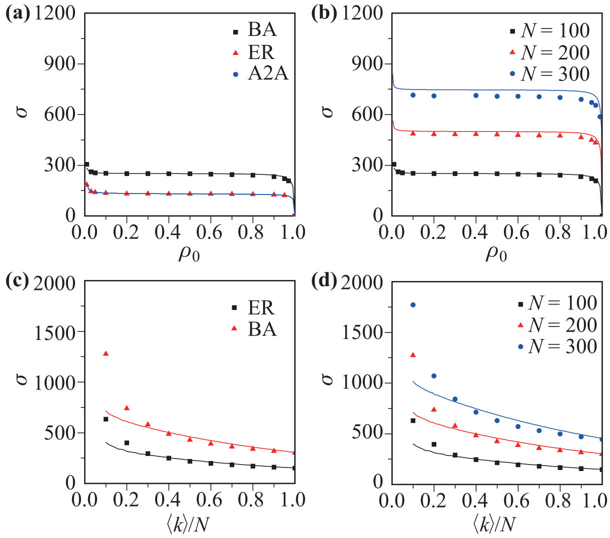

Fig. 7 σ for prisoner's dilemma games versus **(a, b)** initial conditions of ρ_0 and **(c, d)** average degrees $\langle k\rangle$ of networks. (a, c) The network sizes are $N = 100$ for both ER and scale-free networks, and (b, d) three different network sizes for BA networks: (100 (■), 200 (▲), and 300 (●)).

to characterize the evolutionary processes. In the case of coordination games, $\langle t\rangle$ shows large deviations when the initial frequencies of one strategy are close to the unstable interior fixed point. Based on the mean-field assumption, we have obtained explicit expressions for the probability distribution functions of fixation times P_t. More importantly, all m-order moments of the distribution functions are derived. In the numerical simulations, we focused on the standard deviations depending on the initial frequency of one strategy ρ_0 and the average connectivity $\langle k\rangle/N$. When increasing the average network degrees, the results are convergent to the case of all-to-all connections. The difference between the theoretical mean fixation time and the numerical simulation is due to the connectivity heterogeneity, which is typical for scale-free networks. It shows large deviations when the average network degrees are small.

Although our discussions are focused on pairwise comparison processes, our results can be easily generalized to Moran processes. At each discrete time step of Moran processes, an individual is chosen randomly from the population for reproduction proportional to its fitness, and another individual is chosen at random for death and replaced by the new offspring. In this case, we have two slightly different ways of replacing neighbors when the offspring is produced; in particular, either in the neighborhood of the chosen player or in the whole network. Our theory relies on a mean-field approximation; therefore, it works slightly better if the replacing takes place on the network-wide scale. A more systematic analysis of the replacing rules will be done in future work. One of more challenging tasks is to generalize the present investigation from one structured population to two interacting (coupled) populations, where more interesting dynamic behaviors will be observed [38].

Acknowledgements This work was in part financially supported by the National Natural Science Foundation of China (Grant Nos. 11305062, 11405059, and 11575041), and the Natural Science Foundation of Shanghai (Grant No. 17ZR1444800).

Appendix A Transition matrix M

The transition matrix of the evolutionary process is obtained as

$$\begin{aligned} M &= \begin{pmatrix} 1 & 0 & 0 & 0 & \cdots & 0 \\ T_-(1) & T_0(1) & T_+(1) & 0 & & 0 \\ 0 & T_-(2) & T_0(2) & T_+(2) & & 0 \\ \vdots & & & & \ddots & \vdots \\ 0 & 0 & 0 & 0 & \cdots & 1 \end{pmatrix} \\ &= \begin{pmatrix} I_2 & 0 \\ R & Q \end{pmatrix}, \end{aligned} \tag{A1}$$

where

$$I_2 = \begin{pmatrix} 1 & 0 \\ 0 & 1 \end{pmatrix}, \quad R = \begin{pmatrix} T_-(1) & 0 \\ 0 & 0 \\ \vdots & \vdots \\ 0 & T_+(N-1) \end{pmatrix},$$

$$Q = \begin{pmatrix} T_0(1) & T_+(1) & 0 & \cdots & \\ T_-(2) & T_0(2) & T_+(2) & & \\ \vdots & & & \ddots & \vdots \\ 0 & 0 & 0 & \cdots & T_0(N-1) \end{pmatrix}; \tag{A2}$$

I_2 represents the two absorbing states, R is the probability for the system to reach the absorbing states in 1 step, and Q is the transition probabilities for any transient states. We further denote the following two matrices

$$H = (I_{N-1} - Q)^{-1} \tag{A3}$$

$$= \begin{pmatrix} T_+(1)+T_-(1) & -T_+(1) & 0 & \cdots & \\ -T_-(2) & T_+(2)+T_-(2) & -T_+(2) & & \\ \vdots & & & \ddots & \vdots \\ 0 & 0 & 0 & \cdots & T_+(N-1)+T_-(N-1) \end{pmatrix}^{-1}, \tag{A4}$$

$$B = HR = \begin{pmatrix} H_{11}T_-(1) & H_{1(N-1)}T_+(N-1) \\ H_{21}T_-(1) & H_{2(N-1)}T_+(N-1) \\ \vdots & \vdots \\ H_{(N-1)1}T_-(1) & H_{(N-1)(N-1)}T_+(N-1) \end{pmatrix}. \tag{A5}$$

Note that the matrix $I_{N-1} - Q$ is tridiagonal, the inverse of which determines the stochastic dynamics of the system, namely, the fixation probabilities and the average times necessary for the system to reach the absorbing states [12, 19]. More specifically, starting from any initial state $S_I(0)$, $I \in [1, N-1]$, we have probabilities of B_{n2} and B_{n1} that the system is attracted to the absorbing states of, respectively, all s_1 players and all s_2 players. The two probabilities B_{n2} and B_{n1} fulfill the normalization

$$\sum_{j=1}^{2} B_{nj} = 1. \tag{A6}$$

Furthermore, the mean fixation time for the system to be attracted to the absorbing state from any initial state of n s_1-players is given by

$$\langle t_n \rangle = \sum_{m=1}^{N-1} H_{nm}. \tag{A7}$$

For the purpose of comparison between networks of different sizes, one normalizes this by the number of nodes in the network, namely, $\langle t_n \rangle / N$.

With the notations of Eqs. (A3) and (A5), the fundamental matrix H of the stochastic process is $H = (I_{N-1} - Q)^{-1}$, where I_{N-1} is the identity matrix of dimension $N-1$ [19].

References

1. J. M. Smith, Evolution and the Theory of Games, Cambridge: Cambridge University Press, 1982
2. J. Hofbauer and K. Sigmund, Evolutionary Games and Population Dynamics, Cambridge: Cambridge University Press, 1998
3. M. A. Nowak and R. M. May, Evolutionary games and spatial chaos, *Nature* 359(6398), 826 (1992)
4. M. A. Nowak, A. Sasaki, C. Taylor, and D. Fudenberg, Emergence of cooperation and evolutionary stability in finite populations, *Nature* 428(6983), 646 (2004)
5. E. Lieberman, C. Hauert, and M. A. Nowak, Evolutionary dynamics on graphs, *Nature* 433(7023), 312 (2005)
6. B. Ottino-Loffler, J. G. Scott, and S. H. Strogatz, Takeover times for a simple model of network infection, http://biorxiv.org/content/early/2017/02/03/105585.full.pdf
7. M. A. Nowak, Five rules for the evolution of cooperation, *Science* 314(5805), 1560 (2006)
8. G. Szabó and G. Fáth, Evolutionary games on graphs, *Phys. Rep.* 446(4–6), 97 (2007)
9. A. Arenas, A. Díaz-Guilera, J. Kurths, Y. Moreno, and C. S. Zhou, Synchronization in complex networks, *Phys. Rep.* 469(3), 93 (2008)
10. C. Taylor, D. Fudenberg, A. Sasaki, and M. A. Nowak, Evolutionary game dynamics in finite populations, *Bull. Math. Biol.* 66(6), 1621 (2004)
11. A. Traulsen and C. Hauert, Stochastic evolutionary game dynamics, in: H.-G. Schuster (Ed.), Reviews of Nonlinear Dynamics and Complexity, Vol. 2, Wiley-VCH Verlag GmbH & Co. KGaA, 2009, pp 25–61
12. N. van Kampen, Stochastic Processes in Physics and Chemistry, 3rd Ed., Amsterdam: Elsevier, 2007
13. T. Antal and I. Scheuring, Fixation of strategies for an evolutionary game in finite populations, *Bull. Math. Biol.* 68(8), 1923 (2006)
14. D. Zhou and H. Qian, Fixation, transient landscape, and diffusion dilemma in stochastic evolutionary game dynamics, *Phys. Rev. E* 84(3), 031907 (2011)
15. T. Galla, Imitation, internal absorption and the reversal of local drift in stochastic evolutionary games, *J. Theor. Biol.* 269(1), 46 (2011)
16. A. Traulsen, J. C. Claussen, and C. Hauert, Coevolutionary dynamics: From finite to infinite populations, *Phys. Rev. Lett.* 95(23), 238701 (2005)
17. A. Traulsen, M. Nowak, and J. Pacheco, Stochastic dynamics of invasion and fixation, *Phys. Rev. E* 74(1), 011909 (2006)
18. M. Mobilia, Stochastic dynamics of the prisoner's dilemma with cooperation facilitators, *Phys. Rev. E* 86(1), 011134 (2012)
19. L. Y. Zhang, Y. Zou, S. G. Guan, and Z. H. Liu, Analytical description for the critical fixations of evolutionary coordination games on finite complex structured populations, *Phys. Rev. E* 91(4), 042807 (2015)
20. M. Assaf and M. Mobilia, Large fluctuations and fixation in evolutionary games, *J. Stat. Mech.: Theory and Experiment* 2010(09), P09009 (2010)
21. M. Assaf, M. Mobilia, and E. Roberts, Cooperation dilemma in finite populations under fluctuating environments, *Phys. Rev. Lett.* 111(23), 238101 (2013)
22. A. J. Black, A. Traulsen, and T. Galla, Mixing times in evolutionary game dynamics, *Phys. Rev. Lett.* 109(2), 028101 (2012)
23. A. Traulsen, J. C. Claussen, and C. Hauert, Stochastic differential equations for evolutionary dynamics with demographic noise and mutations, *Phys. Rev. E* 85(4), 041901 (2012)
24. T. Antal, S. Redner, and V. Sood, Evolutionary dynamics on degree-heterogeneous graphs, *Phys. Rev. Lett.* 96(18), 188104 (2006)
25. K. Hashimoto and K. Aihara, Fixation probabilities in evolutionary game dynamics with a two-strategy game in finite diploid populations, *J. Theor. Biol.* 258(4), 637 (2009)
26. K. H. Z. So, H. Ohtsuki, and T. Kato, Spatial effect on stochastic dynamics of bistable evolutionary games, *J. Stat. Mech.: Theory and Experiment* 2014(10), P10020 (2014)
27. P. M Altrock and A. Traulsen, Fixation times in evolutionary games under weak selection, *New J. Phys.* 11(1), 013012 (2009)
28. T. G. Mattos, C. Mejía-Monasterio, R. Metzler, and G. Oshanin, First passages in bounded domains: When is the mean first passage time meaningful? *Phys. Rev. E* 86(3), 031143 (2012)

29. P. Ashcroft, A. Traulsen, and T. Galla, When the mean is not enough: Calculating fixation time distributions in birth-death processes, *Phys. Rev. E* 92(4), 042154 (2015)
30. Y. Zou, T. Pereira, M. Small, Z. H. Liu, and J. Kurths, Basin of attraction determines hysteresis in explosive synchronization, *Phys. Rev. Lett.* 112(11), 114102 (2014)
31. S. F. Ma, H. J. Bi, Y. Zou, Z. H. Liu, and S. G. Guan, Shuttle-run synchronization in mobile ad hoc networks, *Front. Phys.* 10(3), 343 (2015)
32. X. Huang, J. Gao, Y. T. Sun, Z. G. Zheng, and C. Xu, Effects of frustration on explosive synchronization, *Front. Phys.* 11(6), 110504 (2016)
33. C. Q. Wang, A. Pumir, N. B. Garnier, and Z. H. Liu, Explosive synchronization enhances selectivity: Example of the cochlea, *Front. Phys.* 12(5), 128901 (2017)
34. H. B. Chen, Y. T. Sun, J. Gao, C. Xu, and Z. G. Zheng, Order parameter analysis of synchronization transitions on star networks, *Front. Phys.* 12(6), 120504 (2017)
35. J. Zhang, Y. Z. Yu, and X. G. Wang, Synchronization of coupled metronomes on two layers, *Front. Phys.* 12(6), 120508 (2017)
36. G. Szabó and C. Tőke, Evolutionary prisoner's dilemma game on a square lattice, *Phys. Rev. E* 58(1), 69 (1998)
37. P. P. Li, J. H. Ke, Z. Q. Lin, and P. M. Hui, Cooperative behavior in evolutionary snowdrift games with the unconditional imitation rule on regular lattices, *Phys. Rev. E* 85(2), 021111 (2012)
38. L. Y. Zhang, L. M. Ying, J. Zhou, S. G. Guan, and Y. Zou, Fixation probabilities of evolutionary coordination games on two coupled populations, *Phys. Rev. E* 94(3), 032307 (2016)